

RESEARCH ARTICLE

10.1002/2017JC013419

Special Section:

The Southern Ocean Carbon and Climate Observations and Modeling (SOCCOM) Project: Technologies, Methods, and Early Results

Key Points:

- SOCCOM is deploying biogeochemical profiling floats in the Southern Ocean
- The SOCCOM ensemble is surviving at roughly the same rate as a larger group of Argo floats

Correspondence to:

S. C. Riser,
riser@ocean.washington.edu

Citation:

Riser, S. C., Swift, D., & Drucker, R. (2018). Profiling floats in SOCCOM: Technical capabilities for studying the Southern Ocean. *Journal of Geophysical Research: Oceans*, 123, 4055–4073. <https://doi.org/10.1002/2017JC013419>

Received 31 AUG 2017

Accepted 28 FEB 2018

Accepted article online 23 MAR 2018

Published online 28 JUN 2018

Profiling Floats in SOCCOM: Technical Capabilities for Studying the Southern Ocean

Stephen C. Riser¹ , Dana Swift¹, and Robert Drucker¹

¹School of Oceanography, University of Washington, Seattle, WA, USA

Abstract We report on profiling float technology used in the Southern Ocean Carbon and Climate Observations and Models (SOCCOM) program, a 6 year study of the interaction of ocean physics and the carbon cycle in the Southern Ocean. A central part of this program is to produce and deploy 200 profiling floats equipped with CTD units and chemical sensors capable of measuring dissolved oxygen, nitrate, pH, chlorophyll fluorescence, and particulate backscatter. The performance of the first 63 floats deployed in SOCCOM is examined, and examples of the design criteria used in producing these floats are shown. Some of the sensors require surface measurements to be made in the dark at regular intervals, and the probability of ascending to the sea surface in the dark is estimated as a function of year-day and latitude. An energy budget derived from laboratory measurements shows that only about 25% of the total energy stored in the batteries is used by the biogeochemical sensors, which bodes well for the long-term survivability of the floats. The ice-avoidance algorithm is discussed in detail, and it is shown that it is working as designed and allowing unprecedented numbers of profiles to be collected beneath the wintertime ice cover. The overall reliability of the first group of SOCCOM floats is compared with a much larger ensemble of Argo floats; the results show that the SOCCOM floats are surviving at a rate similar to the Argo floats, which have been shown to have lifetimes in excess of 5 years.

1. Introduction

The use of subsurface, freely drifting floats dates from the 1950s, with their use tied to the discovery of oceanic eddies in the western N. Atlantic by Swallow (1955, 1971) and the observation of the deep western boundary current there by Swallow and Worthington (1957). These early floats were tracked acoustically from a nearby ship, using acoustic frequencies of ~10 KHz; later incarnations of this technology were employed by Swallow et al. (1974) to track more eddies in greater detail. The acoustic tracking technique was expanded and improved by Rossby and Webb (1970) and Rossby et al. (1986) by employing lower acoustic frequencies (~260 Hz) with land-based or moored sound sources, greatly increasing the acoustic range and mission duration. In the 1980s, as part of the World Ocean Circulation Experiment (WOCE), Davis et al. (2001) designed and deployed a new type of non-acoustic float capable of profiling from a relatively deep level (1,000 m) to the sea surface at intervals of weeks to months, with missions lasting several years; data were transmitted through the Service ARGOS satellite system. The WOCE versions of these floats were designed to observe the 1,000 m velocity directly from the surfacing end points between profiles, so that the absolute flow at one level in the ocean could be estimated globally, with the resulting data yielding unprecedented glimpses of the global ocean circulation (e.g., Davis, 2005; Lavender et al., 2000).

Near the end of WOCE the capabilities of these floats were significantly expanded by including the acquisition of a profile of temperature as a function of pressure during the ascent phase of a profile, which was then transmitted to shore stations in near-real time while the float was on the surface between cycles. Floats of this design were deployed in significant numbers in the Atlantic and yielded new insight into the formation and distribution of subtropical mode water (Kwon & Riser, 2005) and flow near the Equator (Molinari et al., 1999). With the advent of temperature profiles, there was immediately an interest in adding the capability of measuring salinity, although this proved to be considerably more problematic. Early deployments that used inductive-style conductivity sensors were fraught with technical problems, including a lack of stability over time. Most of these issues were solved through the use of CTD (conductivity, temperature, and depth) units that employed an enclosed, pumped system with a biocide, with the electrical conductivity of a seawater sample measured directly.

Having the capability to make reliable temperature and salinity measurements from profiling floats was an essential requirement for allowing the Argo program to begin in 1999. The SeaBird 41 CTD employed on the early floats is similar to the CTD unit that is used on nearly all profiling floats today, with some modifications made allowing more rapid sampling in order to take advantage of the faster communications that were not available at the onset of Argo. Since 2007 the Argo array has been populated by over 3,000 floats, with well over one million profiles of temperature and salinity collected and over 3,000 papers published that use the Argo results in some way; the same year marked the first deployment of University of Washington (UW) Argo floats in the Southern Ocean region equipped with Iridium communications and ice-avoidance software. As noted in Riser et al. (2016), the success of Argo has led to an expansion in float capabilities and a number of new research avenues that employ profiling floats. One of these new directions is the use of biogeochemical (BGC) sensors on floats in order to observe various aspects of the biological pump and the oceanic carbon cycle. The use of such floats in the Southern Ocean is the topic of this paper and forms the observational basis of the Southern Ocean Carbon and Climate Observations and Models (SOCCOM) project, which aims to deploy some 200 floats equipped with BGC sensors over a 6-year period to study carbon uptake and export in the Southern Ocean. Initial scientific results from SOCCOM will be discussed in works throughout this collection of papers. Here, we summarize the operation of SOCCOM floats and their technical capabilities, including the details of their basic operation, their CTD sensors and other sensor types, their success rates, batteries and power considerations, communications, and potential new capabilities in the future.

2. Float Data

The focus of this paper is to describe the technology and performance of floats in SOCCOM; the first deployments of such floats began with 10 prototype SOCCOM floats in 2014, with the full SOCCOM program beginning a year later. We focus here on an ensemble of 63 SOCCOM-type floats deployed since 2014 that provided 3,539 profiles in the Southern Ocean through March of 2017. Many of these floats spent parts of several austral winters under sea ice (1,201 of the profiles from these floats, or 34%, were collected under ice). The normal Argo suite of temperature, salinity, and pressure data, as well as observations of dissolved oxygen, nitrate, and chlorophyll backscatter were collected on nearly all of these profiles, and pH data were available from many of the floats that were deployed after mid-2015, when the development and testing of the first version of the sensor was completed (described in detail in Johnson et al., 2016). In addition to the SOCCOM float data, for comparison purposes we have examined in some instances (notably in §7 below) the performance of 99 standard Argo floats (e.g., that collected CTD data only) that since 2007 provided observations both in and out of sea ice in the Southern Ocean (shown in Figure 1), and 373 standard Argo floats from the global ocean that employed Iridium communications (these two groups of standard Argo floats collectively completed 12,139 profiles); the year 2007 was the first year when Iridium-equipped UW floats were first deployed in the sea ice zone. These data were used in order to be able compare the longevity of the technologically more complex SOCCOM floats, which carry multiple sensors, to the simpler and more ubiquitous floats used in Argo. All of the Argo and SOCCOM float data used here are available for direct download from the Argo Global Data Assembly Center (<http://www.coriolis.eu.org/Observing-the-Ocean/ARGO>) and have been archived with a digital object identifier (<http://doi.org/10.17882/42182#47708>).

3. Basic Float Operation

3.1. Buoyancy Engine

Profiling floats cycle vertically at regular intervals by altering their buoyancy, collecting profiles of various oceanic variables during their ascent. The float buoyancy can be examined by noting that

$$M = \rho_o V_o; \quad dM = d(\rho V) = 0. \quad (1)$$

Here M is the mass of the float, which does not change during operation, with ρ_o and V_o the initial float density and volume, and ρ and V the values at any later time. The density and volume vary, thus allowing the float to cycle vertically. Expanding (1), it is found that

$$V d\rho + \rho dV = 0,$$

yielding

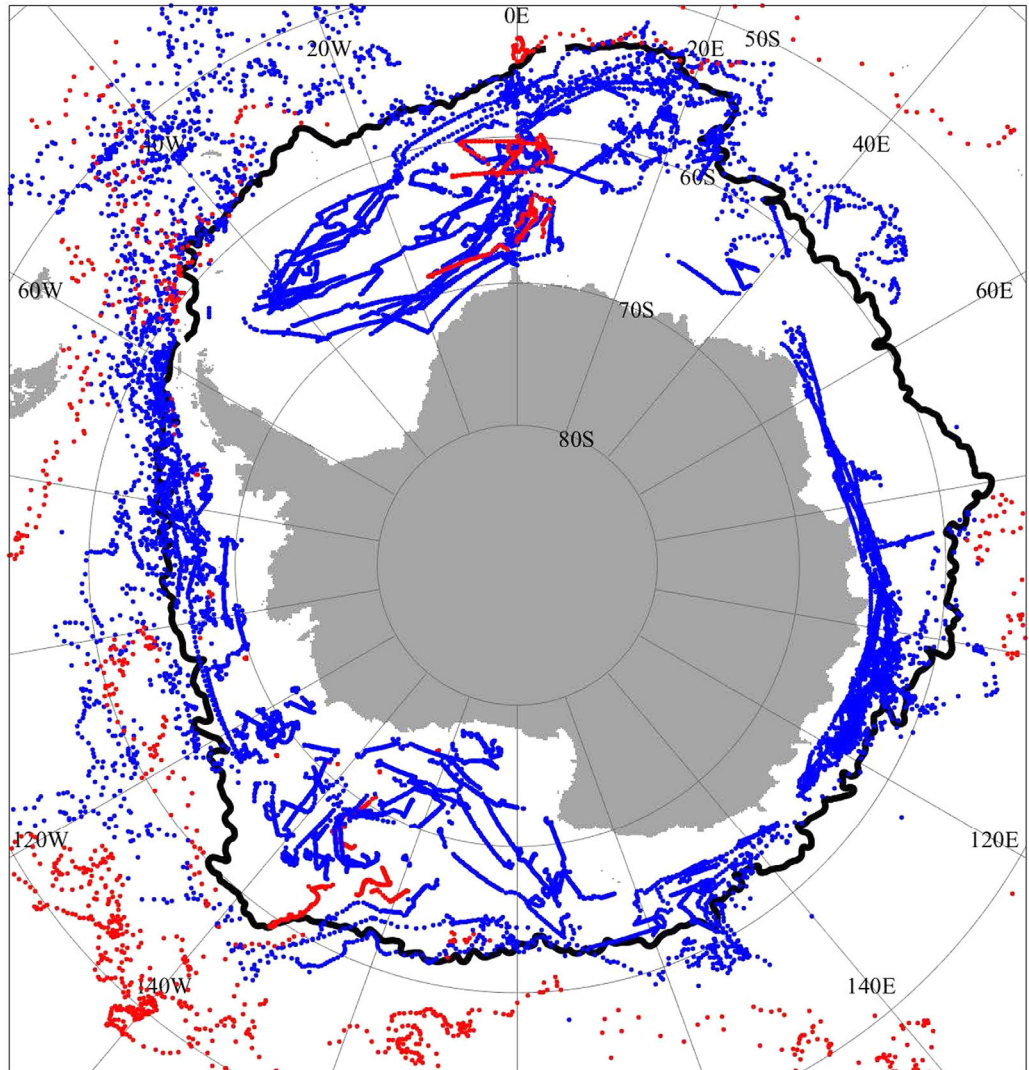


Figure 1. A polar projection map of the Southern Ocean, showing the locations of a portion of the float profile data used in this paper. Blue dots indicate profiles from 99 standard Argo floats collected during the period 2007–2016. Red dots show the locations of profiles from 63 SOCCOM floats collected during the 2014–2016. The solid black line denotes the climatological mean maximum extent of the wintertime ice cover. Profile locations under sea ice are linearly interpolated using the last known autumn position and first surfacing position in the spring, as described in the text. In addition to these two data sets, data from an ensemble of 373 Argo standard Argo floats from the global ocean outside of the sea ice zone (not shown) are used in some comparisons.

$$\lambda = \frac{d\rho}{\rho} = -\frac{dV}{V}. \quad (2a)$$

Formally, from (2a), we can write that

$$\lambda_1 = \frac{d\rho}{\rho}; \quad \lambda_2 = -\frac{dV}{V}; \quad \lambda_1 = \lambda_2. \quad (2b)$$

Since the ocean is vertically stratified in density, varying the float density will cause the instrument to ascend or descend through the water column. From (2b), λ_1 is a parameter that reflects the degree of oceanic stratification, which can be estimated from in situ measurements, as from Argo or data in the Boyer et al. (2013). Also from (2b), λ_2 can be seen to measure the degree to which a float can change its buoyancy based on its engineered characteristics. While λ_1 and λ_2 are formally equal from (2a) and (2b), for a float to successfully cycle between 2,000 m and the sea surface, it is necessary that in actuality $\lambda_2 > \lambda_1$.

We can write an approximate version of (2) that takes into account finite changes in ρ and V as

$$\lambda \approx \frac{\Delta\rho}{\rho_o} = -\frac{\Delta V}{V_o}, \quad (3)$$

where $\Delta\rho$ and ΔV represent the changes in *in situ* density and volume between some depth/pressure level (usually chosen to be 2,000 m) and the sea surface and ρ_o and V_o are the density and volume at that reference level. Profiling floats change their volume in two ways. In the first, an external bladder is inflated with oil at the beginning of a cycle while the float is at depth, changing the float's volume displacement by an amount ΔV_b and the resulting float density by a corresponding amount $\Delta\rho_b$. The fact that the float hulls are themselves slightly compressible (less than seawater) and expand slightly with increasing temperature provides the second method for changing the float volume, denoted by ΔV_h . The float density change $\Delta\rho_h$ due to its hull characteristics can be modeled as

$$\Delta\rho_h = \rho_o(1 - \alpha\Delta T + \gamma\Delta p), \quad (4)$$

where α is the bulk thermal expansion coefficient of the float and γ is the bulk float compressibility, and ΔT and Δp are the changes in temperature and pressure seen by the float. Thus, from (3) and (4) we can write that

$$\frac{\Delta\rho_h}{\rho_o} = -\frac{\Delta V_h}{V_o} = 1 - \alpha\Delta T + \gamma\Delta p. \quad (5)$$

The total relative change in density that is possible is then given by the sum of the effects of bladder inflation and hull variation,

$$\lambda = \frac{\Delta\rho}{\rho_o} = -\frac{\Delta V_b}{V_o} + 1 - \alpha\Delta T + \gamma\Delta p. \quad (6)$$

To ascend from 2,000 m, a float will inflate its bladder ($\Delta V_b > 0$), thus decreasing its pressure ($\Delta p < 0$), and changing its temperature ($\Delta T > 0$ in the tropics and subtropics; often $\Delta T < 0$ at higher latitudes); the net result of these effects will be a decrease the density of the float, based on (6). The relative density changes in the 0–2,000 m depth interval for several types of floats used in Argo and SOCCOM, with varying hull characteristics and displacements, are summarized in Table 1. Presently most of the floats deployed in SOCCOM have a 48" aluminum hull and are fabricated at the University of Washington from components purchased from Teledyne/ Webb Research. Some BGC-Navis floats purchased from SeaBird Electronics have also been deployed. Both varieties of floats employ a SeaBird CTD unit and a suite of BGC sensors supplied by several manufacturers.

Values of λ_1 estimated using all individual Argo temperature and salinity profiles collected during the period 1999–2016 vary considerably over the world ocean (Figure 2), with larger values at lower latitudes, where the vertical stratification is higher. For a 2,000 m float to ascend all the way to the sea surface at any given

Table 1
The Basic Hull and Buoyancy Parameters for Several Types of Floats Used Deployed in SOCCOM

Float type	V_o (mL)	ΔV_b (mL)	α ($^{\circ}\text{C}^{-1}$)	γ (dbar $^{-1}$)	$\Delta\gamma$ (dbar $^{-1}$)	$\frac{\Delta V_b}{V_o}$	$\frac{\Delta V_h}{V_o}$	$\frac{\Delta V}{V_o}$
APEX (40 in. aluminum)	24,700	248	6.9×10^{-5}	2.4×10^{-6}	$\pm 3.1 \times 10^{-7}$	0.0103	0.0045	0.0148
APEX (48 in. aluminum)	29,900	248	6.9×10^{-5}	2.4×10^{-6}	$\pm 3.3 \times 10^{-7}$	0.0083	0.0045	0.0128
APEX (48 in. carbon fiber)	30,400	248	3.2×10^{-5}	3.8×10^{-6}	$\pm 3.6 \times 10^{-7}$	0.0081	0.0072	0.0153
BGC-Navis	22,200	336	6.9×10^{-5}	2.2×10^{-6}	—	0.0151	0.0041	0.0192

Note. The 40-inch Teledyne/Webb APEX float with aluminum hull, built from components at the University of Washington, is the standard configuration used in non-BGC UW Argo floats. The 48-inch Teledyne/Webb APEX SOCCOM float with aluminum or carbon fiber hull is built from components at the University of Washington. BGC-Navis floats are manufactured by SeaBird Electronics. See the text for explanation of the symbols in the table. All UW APEX floats are ballasted at pressures of up to 1,000 dbar in a pressure vessel at UW. The BGC-Navis floats are ballasted at the SeaBird factory at atmospheric pressure, with a single value of hull compressibility γ used for all SeaBird floats. The values for $\Delta V/V_o$ in this table were derived using typical values for the Southern Ocean at 65°S, where SOCCOM floats are regularly used (i.e., $\Delta p = -2,000$ dbar; $\Delta T = -1^{\circ}\text{C}$; $\rho_o = 1037.2$ kg m $^{-3}$). Seasonal and regional variability yields only minor changes in the estimate of $\Delta V/V_o$ (smaller than the variation due to hull-to-hull differences in compressibility) due to the relatively small effect of thermal expansion of the hulls.

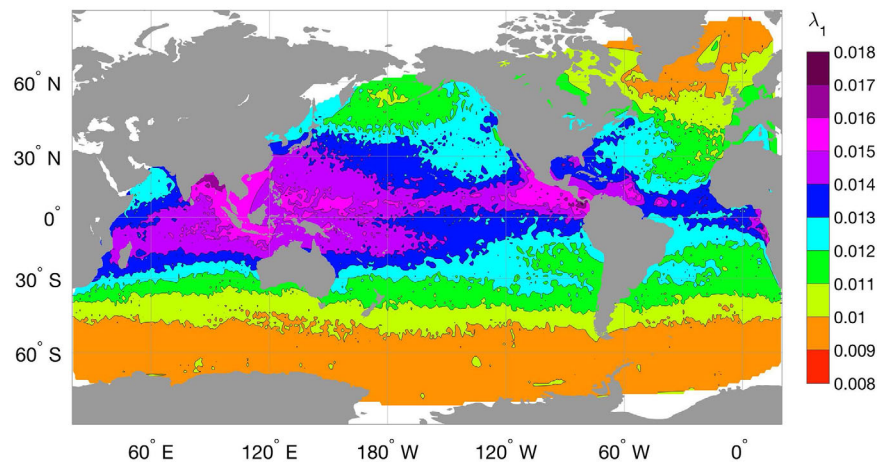


Figure 2. The value of λ_1 for the world ocean between 2,000 m and the sea surface, estimated from the global Argo profile database. The value of λ_2 for a float must exceed this value in order to be capable of profiling to the sea surface.

location, its value of λ_2 as estimated from (6) must exceed the values shown in Figure 2. Based on the values given in Table 1, it is seen that the BGC-Navis floats possess sufficient buoyancy capacity to be able profile from 2,000 m to the sea surface in most regions of the world ocean (except for the Arctic Ocean, which is not considered here). The 48" APEX with a carbon fiber hull can accomplish this in most regions poleward of about 15°, and the 48" aluminum-hulled APEX should be successful poleward of about 30°. South of 40°S, the SOCCOM study region, all of these float types have sufficient buoyancy to complete a 2,000 m profile.

3.2. Ballasting

Equations (1)–(6) provide a framework for designing a vertical cycling protocol for the floats used in SOCCOM and elsewhere. To use these equations, relevant parameters such as the mass and density of the floats as well as the parameters given in Table 1 must be known, requiring individual ballasting of each float. All SOCCOM APEX floats built at UW are ballasted in a high-pressure tank using essentially the same technique described in detail by Swift and Riser (1994). For the UW APEX floats, the mass of each float is determined by using a very accurate laboratory scale that is calibrated daily with a standard mass procured from the National Bureau of Standards; the goal in the laboratory is to determine the mass of each float with an error of less than 1 gram. In the ballast process, each float is put inside a large, freshwater-filled pressure vessel at the UW and subjected to pressures up to 1,000 dbar. The float's density as a function of pressure is monitored by noting the float's position in the vessel; as the pressure is increased, the float will rise in the tank due to the fact that it is less compressible than water. Since the temperature and pressure of the water in the tank are known, the density of the water in the tank is known, so that as the float rises its own density is known; through the use of (1), the float's volume can then be determined as a function of pressure by knowing its mass and density. By measuring the change in volume as a function of pressure, the compressibility γ of each float can be determined, with average values for the different hull types given in Table 1. This procedure allows a determination of the small mass adjustment required for a given float that is necessary in order to have the float park at a given pressure or depth, nominally 1,000 dbar/m. If the value of γ for each hull type were the same for all floats of that type, it would not be necessary to carry out the ballasting operation in the pressure vessel, a time-consuming procedure requiring approximately 1 h per float. However, as can be seen from the column labeled $\Delta\gamma$ in Table 1 (essentially the standard deviation of γ), there is a float-to-float variation in this parameter amounting to about 10% of the mean. Such variations are due to small differences in the machining of the inside diameter of the hulls and cannot be ignored, hence the need to ballast each float individually. The BGC-Navis floats are ballasted at the SeaBird factory at atmospheric pressure, with a single value of hull compressibility used for all floats; this simplification is possible due to the use of a different procedure for machining the hulls, leading to less float-to-float variation in the hull dimensions and compressibility.

3.3. Deployment and Vertical Cycling

Argo-type floats have been deployed from research vessels, ships of opportunity (including fishing boats, sailing vessels, and container ships), and aircraft. To date, SOCCOM float launches have been confined to

research vessels, due to the delicate nature of the sensors on these floats and the need to collect shipboard CTD and chemical data that can be used for sensor calibration. The preferred deployment method is simple and consists of threading a small diameter rope through a hole in the plastic collar of the float, then using the line to lower the float into the water off the stern of the vessel while on station. Once in the water, the line can be pulled back through the hole and the float set free. This technique has been successfully used in a wide range of weather conditions. Recently, some deployments using a protective, biodegradable box containing the float have been carried out; this method is designed for use in harsh weather from vessels with decks especially high above the water line.

Floats are designed to be activated days, weeks, or even months before the expected deployment time. After activation, the instrument software monitors the CTD pressure at 2 h intervals to check if the float has been deployed. If the measured pressure exceeds 25 dbar (a sign that the float is in the water and below the sea surface), the float's mission programming is started; otherwise the float returns to a sleep mode until the next pressure check. Once a float senses that it has been deployed, it enters its *mission prelude* phase, a sequence of events that takes place only around the first profile. In this phase the bladder is fully inflated, returning the float to the surface immediately, where it transmits engineering and scientific data over a period of 6 h. The mission prelude is designed to allow for the possibility of a quick recovery by the deployment vessel if any problems appear with the float. Following the mission prelude, the float adjusts its bladder inflation so that it sinks and becomes neutrally buoyant at a pressure of 1,000 dbar, its eventual parking level. After 5 min at this level the float will execute its first complete profile, returning to the sea surface and transmitting its data. Thus, data for the first profile are available within 24 h of deployment.

Once data from the first profile are successfully transmitted, the float settles into a more regular pattern of vertical cycling and data transmission. There are several segments of the profile cycle, as shown in Figure 3. At the onset of the *descent phase* (T_D in Figure 3), while still at the sea surface (position 1 in Figure 3), the float buoyancy is reduced, causing the float to sink to location 2, its park pressure p_{park} (in Argo and SOCCOM set to be 1,000 dbar). Sinking from position 1 to position 2 requires several hours. Upon reaching position 2, the float enters its *park phase* (T_p), the duration of which is set by the user as part of the mission program, usually 7–10 days long. At the end of the park phase (position 3) the float further reduces its buoyancy and enters the *profile-descent phase* (T_{PD}), where it free-falls until it reaches its deep profile pressure p_{prof} at position 4 (for SOCCOM floats configured to be 2,000 dbar).

After reaching p_{prof} the instrument begins its profile phase (T_U in Figure 3). Inflation of the bladder begins, with regular increments in the degree of inflation until the float reaches the sea surface. This incremental

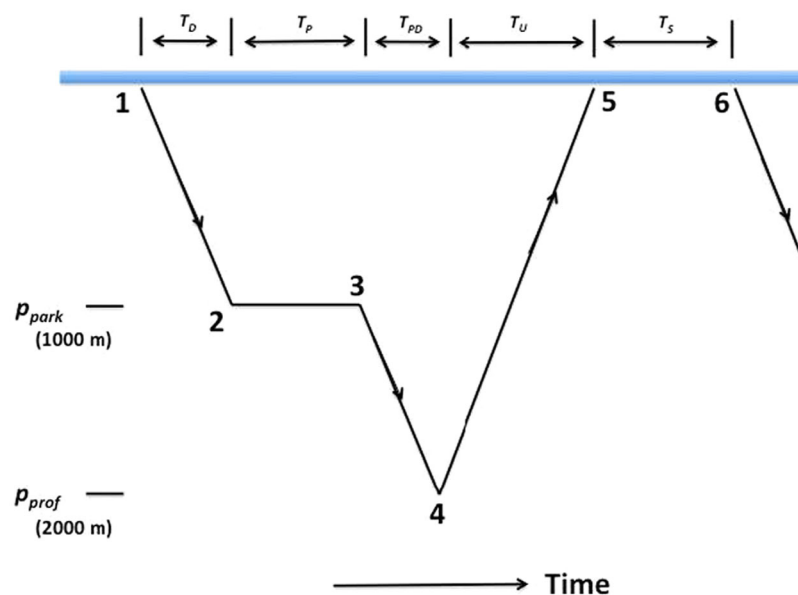


Figure 3. The stages of the cycle of a profiling float over one profile interval, as described in the text.

bladder inflation helps to conserve energy, by carrying out much of the inflation at lower pressures, where the quantity of energy necessary to inflate the bladder is less than at the maximum profile pressure p_{prof} . Incremental inflation also helps to keep the speed of ascent roughly constant throughout the profile, at speeds of 8–10 cm/sec. At such speeds, a float requires 5–7 h to reach the sea surface from 2,000 m.

During the ascent phase T_U , the CTD unit and other float sensors sample the water column at regular intervals and store the data for later transmission. Conductivity, temperature, and pressure are sampled continuously at a rate of 1 Hz over much of the water column as the float ascends; other sensors sample at rates depending on their individual characteristics. By the time a float reaches the sea surface (position 5 in Figure 3), many hundreds of kilobytes of CTD data will have been collected (plus the data from the other sensors), a quantity far too large for cost-effective data transmission. To alleviate this issue, the CTD data from the entire profile are averaged into 2 dbar bins while the float is near the sea surface, shortly before the data are transmitted. In addition to scientific measurements, engineering data relevant to the operation of the float (such as buoyancy parameters, battery voltage, etc.) are collected for later transmission throughout all phases of the float profile cycle.

Once on the surface, floats have four tasks to complete. The first of these, requiring a few minutes, is to collect in-air samples of dissolved oxygen, as described by Johnson et al. (2015); the in-air samples will be used later during shore-based processing to adjust the calibration of the Aanderaa oxygen sensor used on SOCCOM floats. The second task is to acquire a position fix using the Global Positioning System (GPS). This typically requires several minutes of an initial connection between the float and the GPS satellites, followed by a few minutes to determine the position. The third task is to connect with an Iridium satellite and the Iridium gateway, log on to the UW data server, and query the server as to any changes that might be necessary in the mission configuration for the next profile. The fourth and last task is to transmit the profile, surface O_2 samples, GPS, and engineering data via Iridium, which typically requires 5–10 min. Due to interruptions in the transmission process it is often necessary for the data to be transmitted several times before all data have been successfully uploaded. The time on the surface required to complete these three tasks (T_S) typically ranges from 20–30 min. At the end of this period the mission sequence reaches position 6 in Figure 3, where the entire profile cycle begins again. It is expected for SOCCOM floats that this cycle will be repeated 200 or more times.

4. CTD Instrumentation, Other Sensors, and Sampling Protocols

4.1. Basic CTD Operation

Since 2005 nearly all of the floats deployed in the Argo program have been equipped with CTD units manufactured by SeaBird Electronics, Inc. This instrumentation package consists of an electronics unit, CTD pump, and pressure sensor that are located inside the float just below the end cap, with the conductivity cell and temperature sensor located externally inside a tube (see Figure 4). There are two varieties of Sea-Bird CTD instrumentation. In the first (the SeaBird Model 41), values of temperature, conductivity, and pressure (the D , noting the parameter *depth* in the acronym CTD, should actually be p , to represent *pressure*, but the D survives due to historical convention) are spot-sampled at pre-programmed levels during the ascent of the float, with the CTD pump turned off between samples. This is designed to be used when a relatively low vertical sampling rate is required due to data transmission limitations, as when Service Argos satellites are used for data transmission (as in the early days of Argo). For the second form of the SeaBird CTD unit, used on all SOCCOM floats (designated as the Model 41CP, for *continuous profiling*), the CTD pump remains on throughout the profile, allowing samples of temperature, salinity, and pressure to be collected at approximately one-second intervals from 2,000 m to near the sea surface if desired. With the 41CP instrumentation it is possible to mix the continuous and spot-sampling modes. Thus, for the floats used in SOCCOM, the CTD data transmitted on each profile consist of the continuously sampled data binned into 2 dbar intervals at pressure levels above 1,000 dbar, and spot-sampled data at 100 m intervals for levels between 1,000 and 2,000 dbar. The transmitted CTD data stream consists of temperature, pressure, and salinity (computed onboard the float), plus metadata and other engineering data.

The details of the operation of the CTD unit are provided in Riser et al. (2008) and will be only briefly summarized here. During the ascent phase (T_U in Figure 3), the CTD pump draws seawater through the fluid circuit as the float rises. The electrical conductivity (C) of the seawater sample in the cell is measured directly.

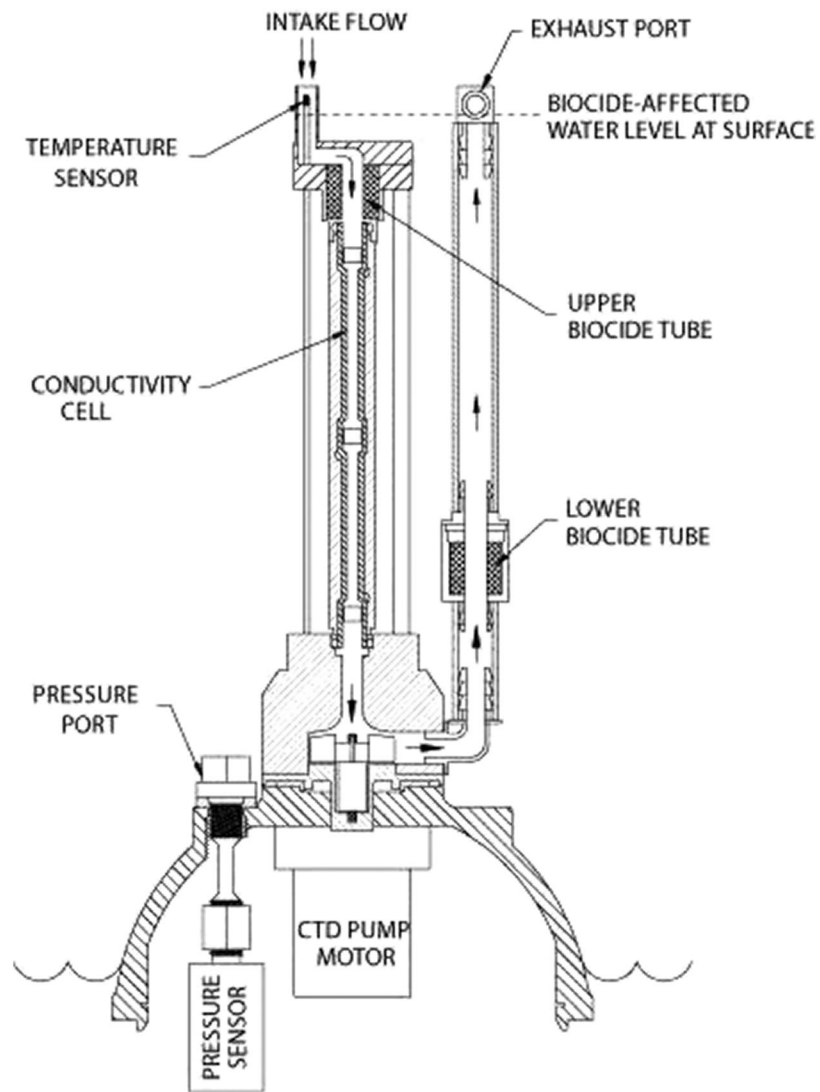


Figure 4. A schematic diagram of a SeaBird 41CP CTD unit. The CTD pump draws seawater through the intake, past the temperature sensor and conductivity cell, and the expels the sample through the exhaust port. Biocide capsules are positioned in both the inflow and outflow in order to inhibit biological growth in the conductivity cell. The pressure sensor is mounted on the float end cap, very near to the CTD unit.

Conductivity, closely related to the reciprocal of electrical resistance R , is estimated by measuring voltage (V) and current (I) in the cell and inferring the resistance (R) using Ohm's Law, $R = V/I$. Since pressure (p) and temperature (T) are measured nearly concurrently with C , salinity S can be estimated on the float via the Practical Salinity Scale (PSS-78) using the known function $S = S(C, T, p)$.

The manufacturer's stated accuracies for S , T , and p are 0.01 (PSS-78), 0.002°C, and 2.5 dbar, respectively. In order to achieve these tolerances, two essential steps must be taken. First, it is noted that estimating C requires a precise knowledge of the geometry of the conductivity cell, which is quite small (a diameter of ~ 1 cm). Even a change in the diameter of the cell of 10^{-4} cm or so over time due to biological fouling can result in undesirable temporal drift in estimates of C and S . To mitigate this potential problem SeaBird installs biocide tablets at the intake and exhaust ports of the CTD cell (shown in Figure 4), effectively prohibiting biological growth in the cell. As a second step to ensure stability over time, the CTD pump is turned off during the ascent phase when the float is at a depth between 2–3 meters. As a result, clogging of the cell from ocean surface water containing various forms of organic and inorganic contaminants is greatly inhibited. Over the years, these design features have worked well, and the CTD sensor accuracy estimates

provided by SeaBird have generally proven to be reliable for Argo-type profiling floats; even for deployments of over 5 years, most floats continue to measure S , T , and p with errors consistent with these limits. Using the methodology of Wong et al. (2003) and Owens and Wong (2009), all UW Argo floats and SOCCOM floats are examined for salinity sensor drift once or twice per year; drifts of the pressure sensor are also examined. For the UW floats data examined in this paper, no more than 10% of the floats required any significant pressure or salinity sensor adjustments, even over deployments lasting many years.

While the floats are drifting in their park phase (noted as T_p in Figure 3, typically about 9 days in duration), the CTD pump and sensors are generally shut off. However, on both Argo and SOCCOM APEX floats a spot sample of temperature is collected once per hour during T_p . These underway records of temperature have proven to be quite useful for studying high-frequency phenomena such as tides and internal gravity waves (Hennon et al., 2014), and it seems likely that other novel uses will be found for these data in the future. For BGC-Navis floats, no underway spot-samples are collected.

4.2. BGC Sensors

The SOCCOM program is designed to examine the biological pump and carbon cycle in the Southern Ocean. Thus, in addition to the standard CTD, most of the floats used in SOCCOM carry sensors capable of measuring O_2 , NO_3 , pH, chlorophyll fluorescence, and particulate backscatter; a few of the early floats did not have pH sensors. The design, details, and performance of each of these sensors to date has been discussed by Johnson et al. (2017) and will not be reiterated here, except to note that in general these sensors are performing well on most floats and their reliability continues to improve due to the evolution of sensor design and technical development as more floats are deployed. The UW-prepared APEX floats used in SOCCOM employ Aanderaa 4330 Optode sensors for O_2 , ISUS NO_3 and pH sensors constructed in-house at MBARI, and FLBB (chlorophyll fluorescence and particle backscatter) sensors purchased from WET Labs, Inc. The BGC-Navis floats purchased from SeaBird use a SeaBird Model 63 O_2 sensor, a Satlantic SUNA NO_3 sensor, and a WET Labs MCOMS unit that measures chlorophyll fluorescence, particulate backscatter, and CDOM. For BGC-Navis floats, some of the pH sensors are produced in-house at MBARI, while others are produced at SeaBird. It is planned that eventually all pH sensors on both APEX and BGC-Navis floats will be fabricated by SeaBird.

The various sensors are mounted on APEX and BGC-Navis floats in different ways. For APEX, the ISUS NO_3 sensor is mounted inside the CTD fluid circuit, while the O_2 and pH sensors are mounted outside of the CTD plumbing on the upper end cap. The FLBB unit is fixed to the outside of the pressure case of the float near the bottom end cap. For BGC-Navis, the O_2 , pH, and MCOMS sensors are mounted inside the fluid circuit, and the SUNA NO_3 sensor is clamped to the outside of the float along its axis, approximately midway between the top and bottom of the cylindrical pressure case. For both float types, the O_2 , NO_3 , chlorophyll fluorescence, and backscatter sensors operate by using the optical properties of seawater at a variety of wavelengths to deduce estimates of the variable in question. The Durafet sensor used on both float types measures pH using electrochemical methods, as discussed in detail by Johnson et al. (2016).

The BGC sensors used on SOCCOM floats have various sampling rates and speeds. In general the desired variables from these sensors are computed onshore once the data have been transmitted; in order to fully estimate the desired quantities, it is necessary to transmit a total of more than 70 measured parameters from each sampled level for the combined sensor suite. As a result, in many cases the BGC variables are sampled at a lower rate than for the basic T , S , and p . For APEX floats, the data stream that results from each profile consists of O_2 , NO_3 , pH, chlorophyll fluorescence, and backscatter sampled at 5 dbar intervals at levels above 100 dbar, 10 dbar intervals at levels between 100 and 400 dbar, and 100 dbar intervals between 1,000 and 2,000 dbar. For BGC-Navis floats, the O_2 and pH sensors are mounted inside the flow cell, allowing the O_2 data to be transmitted at the same intervals as the CTD data (i.e., 2 dbar intervals above 1,000 dbar, and 50 dbar intervals between 1,000–2,000 dbar). For all other variables derived from BGC-Navis data the sampling intervals are 5 dbar intervals above 100 dbar, 10 dbar intervals from 100–400 dbar, and 50 dbar intervals below 400 dbar. The combined CTD and BGC data for each profile are transmitted to a server at UW, where they are distributed to the SOCCOM data center and the US Argo Data Assembly Center at AOML in Miami.

4.3. Vertical Cycling Strategies

The central goal of Argo is to examine the long-term variability in the global heat and freshwater content of the ocean (Riser et al., 2016). In order to accomplish this, the Argo array was designed to sample the climate-scales of variability, essentially horizontal scales of 300 km and greater in space and 10 days and greater in time. Since there is likely important, nonrandom variability on time scales shorter than 10 days (i.e., diurnal variability near the sea surface), it is important to Argo that the 10-day samples be collected throughout all times of the day, so that climate-scale variability estimates are not biased by regional and global effects of diurnal heating and precipitation. This caveat similarly applies to SOCCOM floats, since many of them also serve as Argo floats. On the other hand, most of the BGC sensors on SOCCOM floats operate via optical methods, and the quantity of ambient sunlight present during sampling can in some cases strongly influence the quality of the measurements. As noted by Bushinsky et al. (2016), sunlight-induced errors as large as several percent occur in Aanderaa Optode O₂ sensors, making nighttime sampling and collection of in-air O₂ samples to calibrate the Optodes essential in order to attain the 1% O₂ accuracy desired in SOCCOM. Similarly, daytime chlorophyll fluorescence measurements made from WET Labs FLBB sensors are also biased.

While constraining the floats to sample only in the dark would likely bias near-surface temperature measurements and degrade the data set relevant to Argo, imposing such a constraint is seemingly unnecessary. The work of Johnson et al. (2015), showing the utility of in-air O₂ samples for correcting Aanderaa Optodes, demonstrates that the long-term drift of the sensors (approximately 0.4% per year) is quite slow compared to the nominal 10-day profiling interval, so that it is only necessary to occasionally collect air-O₂ samples in the dark. Since the floats sample at roughly 10-day intervals (this includes a certain degree of randomness, since ascent and descent rates during profiling vary depending on ocean conditions), over time each float will sample at all possible hours of the day. As long as an air sample is collected reasonably often (Bushinsky et al., 2016 suggest at least once per month), the sensor can still likely be adequately calibrated, even though most of the profiles will be collected during hours with nonzero ambient sunlight. At latitudes where daylight intervals are long (high southern latitudes in Austral summer), the time interval between nighttime profiles might be several months long. Conversely, at latitudes where daylight intervals are short or nonexistent (high southern latitudes in Austral winter), the probability of nighttime sampling is very high, although the float might be under sea ice during this period and be unable to collect and air sample or transmit.

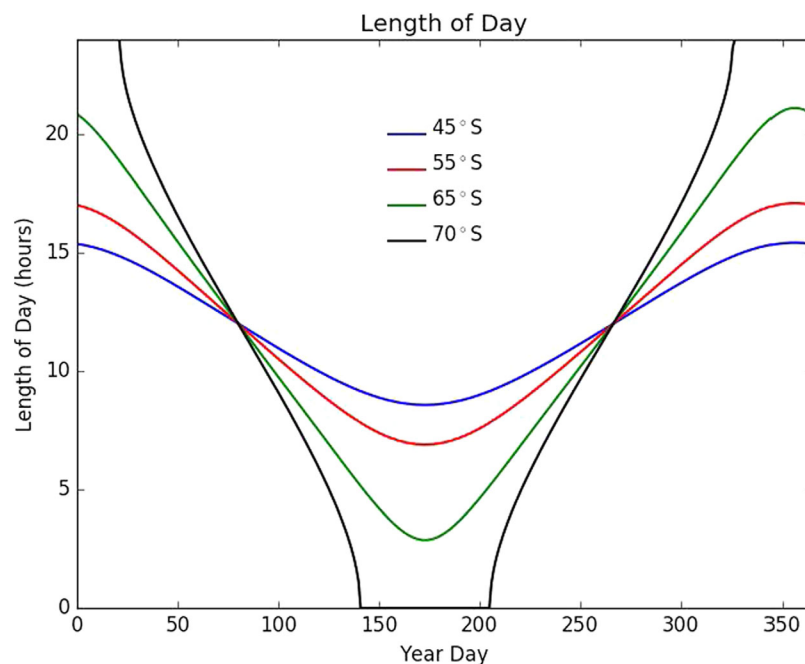


Figure 5. The length of day as a function of year day, defined as 1 h before sunrise to 1 h after sunset, at various latitudes in the Southern Hemisphere. This was derived from the functional formulation given in Iqbal (1983).

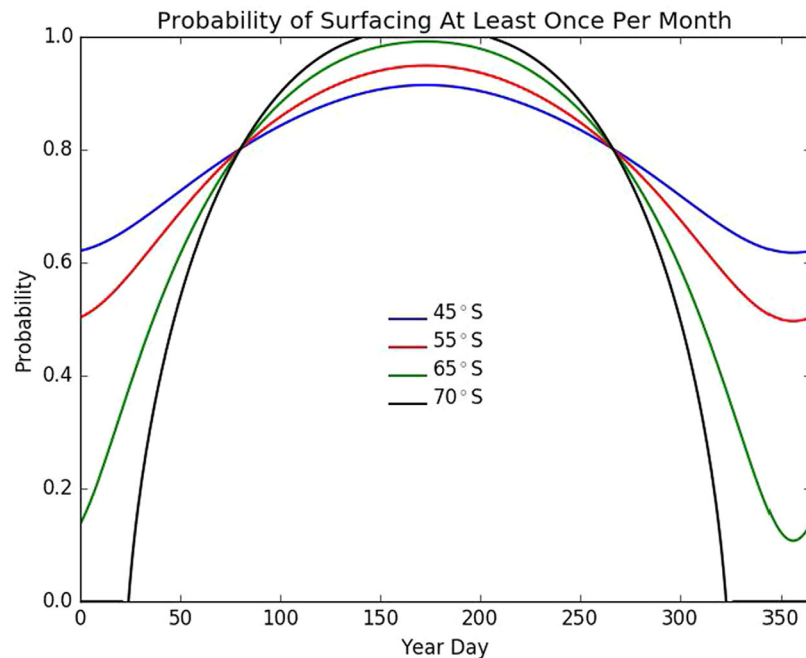


Figure 6. The probability of a float surfacing at least once per month in darkness in the Southern Hemisphere, based on the length-of-day estimates shown in Figure 5. Note that at 65°S and 70°S the ocean is likely ice-covered when the probability is highest, rendering satellite communication impossible.

Some feel for the use of air-O₂ samples obtained by cycling through all times of the day can be seen from an examination of Figure 5. The length of day (defined here as 1 h before sunrise to one hour after sunset) as a function of year-day and latitude is shown, computed using the formulation given in Iqbal (1983). Floats drifting under the wintertime ice (usually south of about 60°S) cannot collect an air sample for O₂ sensor calibration or transmit data in real-time, and at latitudes poleward of about 66°S there is a period of perpetual darkness in winter (approximately days 145–210) and perpetual daylight in summer (approximately day 335 through day 10 in the following calendar year), with equal amounts of day and night at all latitudes around the autumn and spring equinoxes (year days 79 and 350).

Using these length-of-day estimates, it is possible to estimate the probability of surfacing in the dark (defined here as within an hour of local midnight) at least once per month. Letting τ be the length of day (as shown in Figure 5), the probability ε ($0 < \varepsilon < 1$) of surfacing during daytime on any profile is $\tau/24$. If it is supposed that there are n profiles collected in a given month, then the probability ν of getting n profiles during the daytime in a given month is ε^n . Thus, the probability μ of getting *at least one* profile per month in darkness (the converse of getting n consecutive profiles during daytime) is $1-\nu$, or $1-\varepsilon^n$. For most Argo and SOCCOM floats we choose $n = 3$ (profiling at 10-day intervals). The resulting probability μ for $n = 3$ is shown in Figure 6 as a function of latitude and year day, based on the τ values shown in Figure 5. As can be seen in the figure, north of 55°S there is better than a 50% likelihood of collecting at least one profile in the dark in any given month, which should be sufficient for carrying out air calibrations. At higher latitudes ($>66^\circ\text{S}$) the probability in winter is very high (but since the ocean is ice-covered in winter, surfacing is not likely), and very low in summer during perpetual sunlight. Thus there is a narrow range of times during the year (spring and autumn) when the floats will be able to collect dark samples at very high latitudes but the probabilities are quite favorable elsewhere in the SOCCOM region.

5. The Sea Ice Regime

A major feature of the Southern Ocean south of 60–65°S is the seasonal sea-ice cover, as shown in Figure 7. The wintertime ice covering the deep ocean generally disappears by summer except in the Weddell Sea and a few other smaller regions. Examining the physics and chemistry of the ocean in the presence of sea

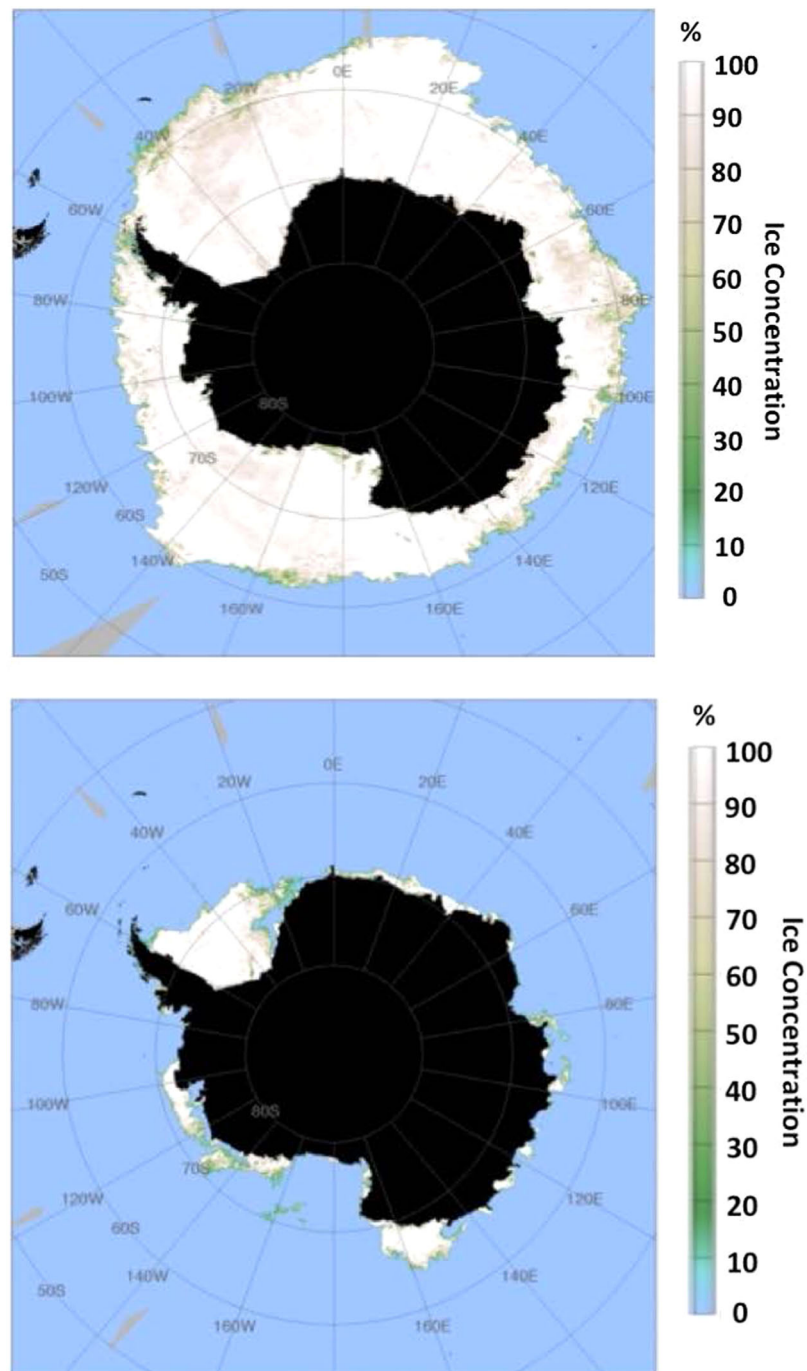


Figure 7. Ice concentration (% cover) for winter and summer in the Southern Ocean, derived from AMSR-E satellite imagery. Top: image from 19 July 2005. Bottom: image from 27 February 2006.

ice is a main focus of SOCCOM, so the floats must be capable of year-round operation in such a regime. It is desirable for the floats to operate normally during periods when no ice is present and to collect and store profiles under the ice at other times of the annual cycle. There are risks to collecting data in the presence of sea ice: floats might be crushed between floes while attempting to transmit their data while on the surface, or they might be damaged by contacting the underside of the pack ice.

There are several possible strategies for operating floats in the ice regime. We have chosen a rather simple solution to this problem, originally suggested by Klatt et al. (2007), which can be implemented using

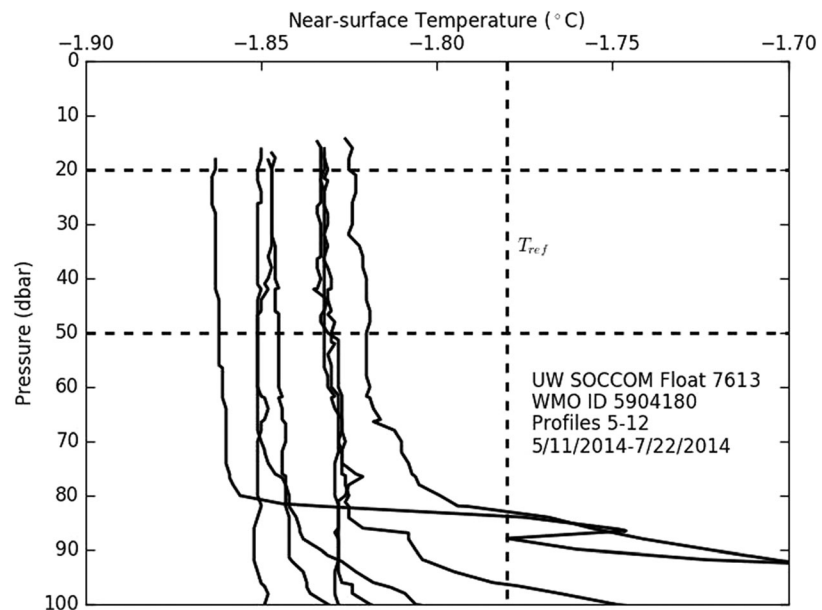


Figure 8. A series of near-surface temperature profiles under sea ice in the Ross Sea, as measured by UW SOCCOM float 7613 (WMO 5904180). The horizontal dashed lines show the region where the median temperature is determined during float ascent. This median temperature is compared to a reference temperature, T_{ref} (shown by the vertical dashed line) on each profile in order to assess whether or not ice cover is likely present.

modifications to the float software, with no additional hardware required for operation in the presence of sea ice. The strategy has been implemented here with some modifications to the original idea and updated for use with Iridium communications, which was not available to the original authors at the time their paper was written. The ice-sensing algorithm used here exploits the notion that in winter, under Antarctic sea ice, there is generally a surface mixed layer (ML) in temperature, salinity, and density that is 100 m or more thick and has a temperature near the freezing point of seawater at the local surface salinity and zero pressure. An example of this can be seen in Figure 8, which shows the near-surface temperature from a number of profiles from a float in the northern Ross Sea in 2014. As can be seen, the temperature between the shallowest point in the profile (a depth of 13–15 meters) and about 80 meters is constant to within about 0.02°C. This is typical of the ML under Antarctic sea ice in mid-winter. The ice-sensing algorithm used on SOCCOM floats simply computes the median temperature T_{med} of the water column between depths of 50 m and 20 m on board the float during ascent (the horizontal dotted lines shown in Figure 8) and compares this to a reference temperature T_{ref} chosen for UW Argo and SOCCOM floats to be -1.78°C (the dotted vertical line in Figure 8). If $T_{med} < T_{ref}$, it is inferred that ice is present above and the float will terminate its ascent, store its profile data, and begin to descend back to its parking depth p_{park} (position 2 in Figure 3) to begin its next cycle. For the profiles shown in Figure 8, the float ascended to within 13–15 meters of the sea surface before it ceased its ascent. A histogram (Figure 9) for all Argo and SOCCOM profiles collected in the presence of sea ice shows that in general floats in this regime will collect data to within a range of 5–25 meters of the sea surface.

A combined histogram (Figure 10) that includes data from over 5,000 profiles (all SOCCOM data and some recent Argo profiles) under ice provides a summary of the performance of the ice algorithm. For about 80% of the under-ice profiles, the results show $T_{med} < T_{ref}$, causing the float ascent to be aborted, the profile data stored, and another cycle initiated. Also shown in Figure 10 is the range of freezing points (T_f) in these profiles (estimated using the Practical Salinity Scale), determined using the measured salinity in the range of 20–50 m at a pressure of zero (the sea surface). It is clear that in general the range of values of the inferred T_f corresponds closely to the range of values for T_{med} , which justifies the basic rationale underlying the Klatt et al. (2007) idea.

From Figure 10, it can also be seen that in about 20% of the profiles $T_{ref} < T_{med}$, even though sea ice was likely present. This occurs mostly in autumn or spring when ice is actively forming or melting and the ice

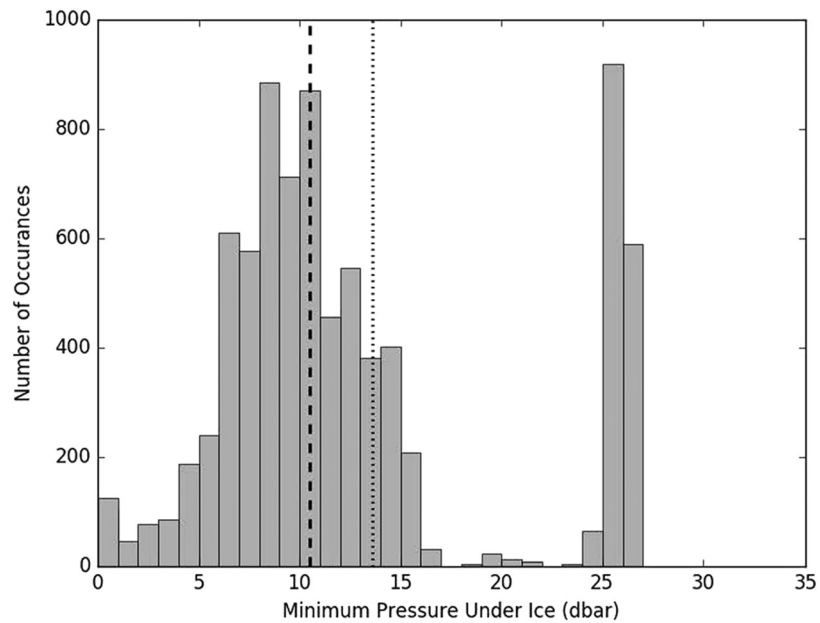


Figure 9. A histogram of the minimum pressure reached by floats under sea ice using the ice-avoidance algorithm described in the text, compiled from 823 profiles collected under ice from Argo and SOCCOM floats from 2007–2016. The bold dashed line denotes the median value, and the dotted line the mean value. The relatively large number of outliers in the range 24–27 dbar are from some of the first floats deployed with the ice algorithm in 2007, when the algorithm was still being refined.

cover is not 100%. In this case the sea ice test fails, and one possible outcome is that the float will continue to ascend until it encounters the underside of the ice. If this occurs, the float will be unable to initiate satellite communications; the ice algorithm for this case is designed so that after several unsuccessful attempts

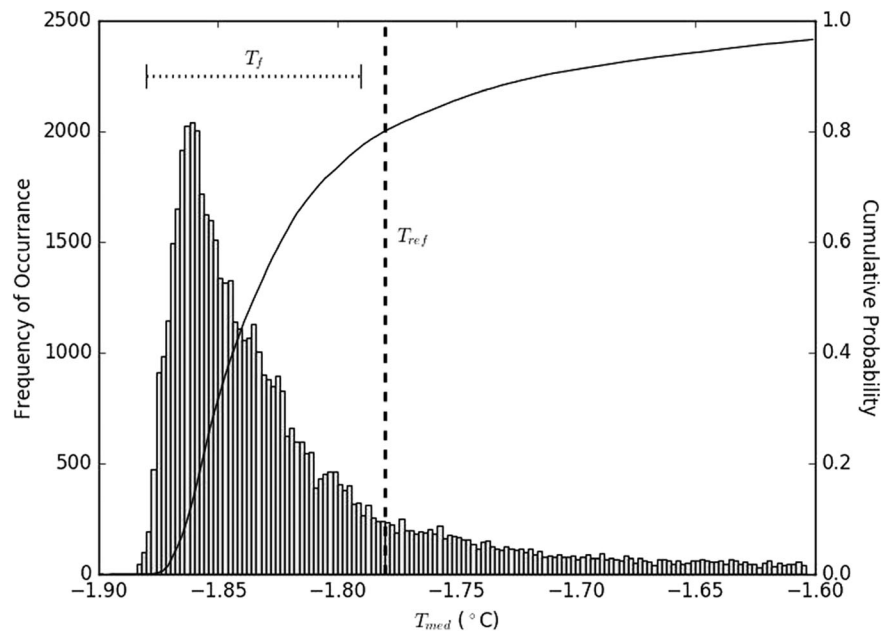


Figure 10. A histogram of the measured median temperature T_{med} for 823 Argo and SOCCOM floats near Antarctic ice during the period 2007–2017. The vertical dashed line shows the reference temperature T_{ref} set by the ice avoidance algorithm. The parameter T_f shows the freezing point temperature inferred for water at the surface based on near-surface measurements of salinity by the floats. As can be seen, in nearly 80% of the winter profiles the temperature of the under-ice mixed layer is less than T_{ref} , implying ice cover above and triggering the end of ascent and storage of the profile.

to connect with the satellite the profile data will be stored and descent to p_{park} for the next profile will be initiated. A second possibility is that $T_{ref} < T_{med}$ and the float actually reaches the sea surface and could potentially communicate with a satellite. However, it is conceivable in this case that ice is still plentiful and the float could be crushed between melting floes. To attempt to prevent this, we require that the float make it to the sea surface and be capable of communicating with a satellite on two successive profiles before allowing the float to stay on the surface and initiate its data transfer. This additional step, requiring a wait of up to 20 days, has the disadvantage of preventing near-surface observations at precisely the time of ice breakup, but in its favor it has allowed UW Argo and SOCCOM floats to survive for multiple years in a seasonal ice-covered regime and to only rarely be damaged by drifting pack ice.

The floats collect and store profile data while under winter ice and transmit the data while on the surface early in the ice-free summer. However, the exact geographic positions of the under-ice profiles are generally unknown since it is impossible to collect GPS fixes through the ice. For some applications, it seems reasonable to simply linearly interpolate the positions to the profile times under the ice using the last GPS fix in the fall and the first fix in the spring. This procedure makes the inherent assumption that the profiles collected by the floats while under the ice represent the properties of the water column at horizontal scales larger than the distance that the float traverses over the winter. In tests using measured summertime positions and particle simulation experiments in models similar to Wang et al. (2014), Chamberlain et al. (2018) found that such interpolation might yield uncertainties of up to 100 km in the estimated location of floats by the end of winter, with the error being cumulative from the period of ice formation to ice melting; some improvement in the linearly-interpolated position estimates can possibly be found using a Kalman filter. Occasionally, it is possible to attempt to actually track the floats under the ice using acoustic methods; beginning in 2007, a suite of 17 UW Argo floats equipped with RAFOS receivers tested this concept by recording acoustic travel times in the Weddell Sea transmitted by an array of 8 moored acoustic sources maintained by colleagues at the Alfred Wegener Institute for Marine and Polar Research in Germany. While long-range ($> 1,000$ km), low frequency (~ 260 Hz) acoustic transmission has been found to be quite reliable at mid-latitudes (Rossby et al., 1986), the results in the Weddell Sea under winter sea ice were considerably poorer, with fewer than 50% of the acoustic transmissions being received even at relatively short ranges, less than 100 km. These difficulties in the ice regime are due to the general lack of a sound channel in the water column at high latitudes as well as the absorption and scattering of the acoustic signals by the ice itself. Chamberlain et al. (2018) has examined these issues in considerable detail and found that for addressing scientific questions related to the large-scale circulation, a precise knowledge of the under-ice positions may not be a strong requirement; for making objective maps of more local under-ice properties or estimating heat and freshwater fluxes, the problem is likely more severe. It is clear that making substantial improvements over linear interpolation under the ice at a reasonable cost will be a difficult undertaking, one that deserves a great deal of thought and experimentation in the future.

6. Satellite Communications and Data Transmission

All floats deployed in SOCCOM, both UW-APEX and SeaBird BGC-Navis, employ the Iridium satellite system for data communications. The communication software used in both types of floats was originally developed at UW in 2004 and has evolved since that time, with the commercial versions of the floats adopting the UW implementation of the Iridium software. There are two general ways that data can be transmitted using Iridium. In the first, known as the Router-Based Unrestricted Digital Internetworking Connectivity Solutions (RUDICS) method, 2-way communication over a circuit-switched data channel is used. While this technique is relatively slow (a throughput of ≤ 300 bytes per second), it is possible to routinely transfer files of 100 kilobytes or more with this method at a reasonable cost. After the data are transmitted from the floats to Iridium, the system initiates a connection to a data server located in the UW float laboratory and the data are automatically downloaded. At the same time, commands from the float operators to alter the float mission can be uploaded over this path back to the float via the Iridium satellites. A second form of Iridium data transmission, Short-Burst Data (SBD), is available for use where the amount of data being transmitted is relatively small and is analogous to sending a text message. While the SBD method has worked well for basic Argo floats where only CTD data are collected, for SOCCOM we exclusively use the RUDICS method via an Iridium 9523 modem inside the float, due to the large quantity of data being transmitted for each profile, as can be seen in Figure 11a.

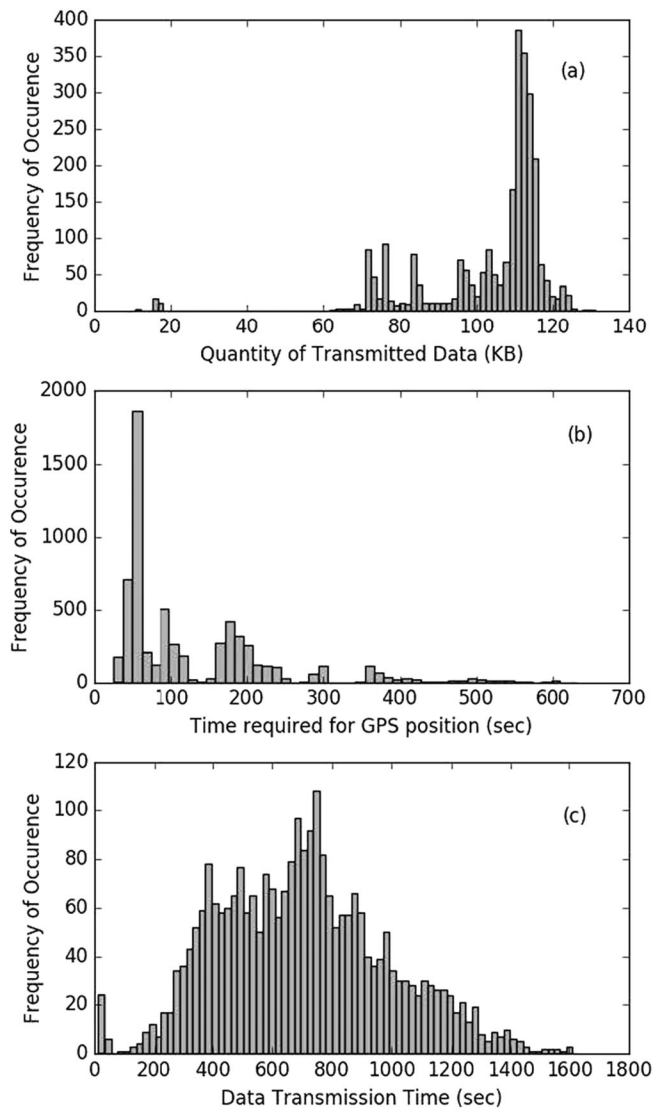


Figure 11. (a) A histogram of the quantity of data transmitted on a given profile for 63 SOCCOM floats. (b) The time required to acquire a GPS position from these SOCCOM floats. (c) The total time spent transmitting data while on the surface for 63 SOCCOM floats.

While on the surface, SOCCOM floats acquire and transmit several GPS fixes, which can require up to several minutes (Figure 11b), then transmit all of the profile, engineering, and positioning data via the Iridium RUDICS protocol. As can be seen from Figure 11c, it is not atypical to spend 10–15 min transmitting data while on the sea surface, with occasional transfers requiring 20–25 min (non-BGC Argo floats upload their data at the same Iridium transfer rate as SOCCOM floats, but the non-BGC floats typically transmit only about 40% as much data per profile, leading to shorter times on the surface). Floats emerging from under sea ice in spring often need to upload 15–20 stored profiles, but, owing to the fixed Iridium transfer rate, the time required to accomplish this is essentially the same as for the same number of profiles transmitted individually by non-ice floats. The variability in the total transmission time is largely due to variations in sea state and weather at the float site, although data transmission has generally been successful in most sea states and weather conditions.

It is possible to alter the float mission using commands from the shore-based laboratory to the float via Iridium. Presently nearly 30 commands are available that can be used to remotely change many of the parameters depicted in Figure 3. It is possible, for example, to alter the duration between profiles with a relatively simple command, or to change the parking depth or maximum profiling depth of a float. If problems occur with a particular float, extra engineering data can be transmitted, the time on the surface can be increased, or the float can be commanded to remain on the surface indefinitely while transmitting at regular intervals, so that it can be recovered. The 2-way communication capability has changed the entire process of data collection from profiling floats and has helped to decrease the losses by allowing the reconfiguration of missions in order to fully exploit all possible environmental scenarios.

7. Energy Considerations and Float Lifetimes

The UW-produced APEX/SOCCOM floats are powered by Electrochem CSC93 lithium battery packs. Each pack consists of 4 DD lithium cells supplying 3.9 volts per cell; each float contains 4 battery packs. With each cell capable of supplying 325 kilojoules (KJ) of energy, a total of 16 cells \times 325 KJ per cell, yielding a total of 5,200 KJ of energy, is available to a float during its mission. Over the course of the mission

this energy will be expended in a number of ways, including operating the basic float buoyancy engine, running the CTD electronics and pump, powering the Iridium communications module and GPS, and running the various BGC sensors on the float. In addition, the batteries will power the basic float electronics (the APF9i controller) that manage and command each of these modules.

In the UW float laboratory we have attempted to quantify each of these energy sinks to the greatest degree possible. To this end, we have tested several SOCCOM-style floats in a small pressure vessel that encloses the oil bladder at high pressure (\sim 1,000 dbar) while exposing the float electronics to the air so that power consumption by the various float systems can be monitored. Through this process we have constructed an energy budget that characterizes the behavior of SOCCOM floats while in the ocean under pressure. From this budget, we can assess the potential lifetime of the floats, assuming that their ultimate failure is caused only by exhaustion of the energy in the batteries. For Argo floats, an energy budget constructed in this fashion has proven to be quite accurate over the course of many multi-year deployments. For SOCCOM, most floats have not yet been in the water long enough to approach their energy-limited lifetimes.

Table 2
An Energy Budget on a Per-Profile Basis for UW-Built SOCCOM APEX Floats, as Discussed in the Text

System	Energy required (KJ)/profile	Percent of total
Buoyancy pump	6.42	32.4
ISUS/NO ₃	3.62	18.3
SeaBird 41CP	3.04	15.3
Iridium-GPS	2.50	12.6
APF9i	1.99	10.0
Durafet pH	1.28	6.5
FLBB	0.16	1.3
Optode/O ₂	0.10	0.5
Self-discharge	0.70	3.5
TOTAL	19.82	100

Note. The term self-discharge refers to the fact that batteries age over time and slowly lose a small amount of energy even if not connected to a load. The values shown have been estimated from direct laboratory measurements under pressure. A total of 5,200 KJ are available in the batteries, yielding an estimate of the float lifetime to be about 262 profiles. Note that during the park phase between profiles (T_p in Figure 3) the APF9i controller is operative, though at a much reduced power level, with the other sensors in this table shut off during that period; the small amount of energy consumed by the APF9i during the park phase is included in the energy estimate given above.

An energy budget for UW-built APEX SOCCOM floats formulated using this method (Table 2) shows that by far the largest consumer of energy over the float lifetime is the buoyancy pump, which must work against pressure to inflate the bladder with oil at a depth of 2,000 m in order for the float to ascend. The second largest energy user is the MBARI-supplied ISUS/NO₃ sensor, which remains on during the entire float profile in order to maintain stability and avoid unwanted transients. To minimize power use, only 70 observations are made on a profile, and the sensor is put in a lower power state between measurements. The SeaBird 41CP CTD unit is the third largest consumer due to the fact that the CTD pump and CTD electronics are kept on for most of the float profile in order to provide continuous CTD data. Iridium communications, GPS activity, and powering the APF9i float controller follow in order of energy use. Near the end of the list are the remaining BGC sensors (pH, FLBB, and oxygen). As can be seen, except for NO₃ the amount of energy consumed by these sensors is relatively small compared to the basic float operations. Overall, energy usage by the BGC sensors accounts for about 25% of the total energy contained in the battery packs. Thus, the floats used in SOCCOM are generally compatible with Argo-type missions and can serve as members of the Argo array as well as sampling BGC variables in SOCCOM.

As noted, each UW-built APEX float with BGC sensors carries a total of 5,200 KJ of energy when deployed. Laboratory measurements under pressure have shown that about 19.82 KJ of energy is expended on each profile; this includes all of the operations of the float and sensor drain as shown in Table 2. This suggests that there should be enough energy in each float to operate for 262 profiles, or over 7 years with a profiling interval of 10 days, although there have not been any SOCCOM floats in the water long enough to confirm this estimate. As can be seen from an examination of Figure 12, however, there is good confirmation for analogous estimates of float lifetime based on the battery energy available for floats deployed in Argo. We have shown the estimated lifetime versus the number of profiles in Figure 12 for the ensemble of 373 standard UW Argo floats deployed since 2007; the Argo

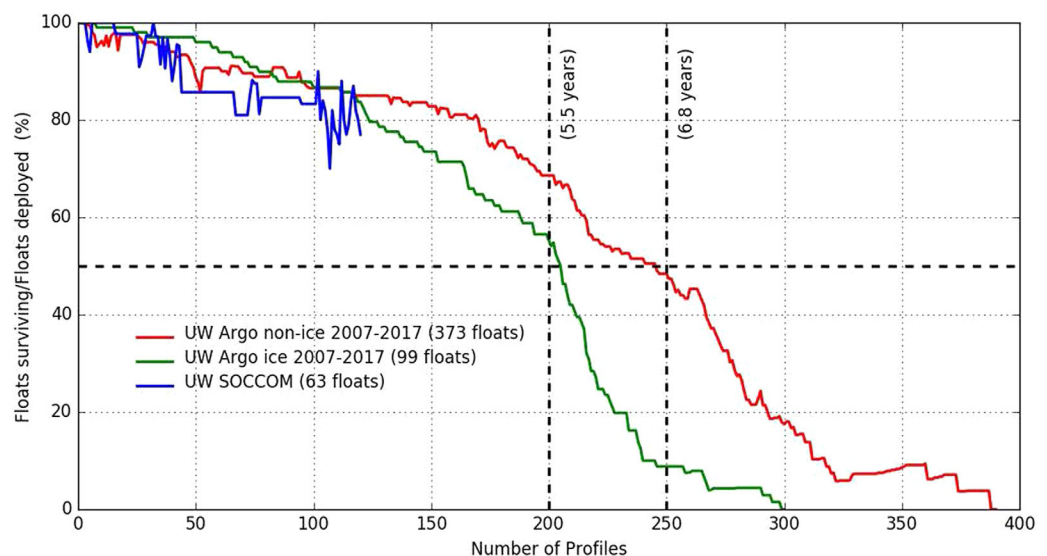


Figure 12. The total number of active floats compared to the number of floats deployed (%) as a function of number of profiles, for ensembles of non-ice Argo floats, Argo floats under sea ice, and SOCCOM floats. The horizontal dashed line denotes a value of 50% while the vertical dashed lines show times of 200 and 250 profiles (5.5 years and 6.8 years at 10-day cycling).

floats used in this study all employed Iridium communications, carried only an SeaBird 41CP CTD with no other sensors present, and operated outside of the sea ice zone. The maximum lifetime for these floats derived from laboratory-based measurements is around 300 profiles (although a few floats continue operating for as long as 400 profiles), and, as can be seen, for this suite of Argo floats about half survived for at least 250 profiles (6.8 years at 10-day sampling), with some operating much longer. The 50% of the floats that ceased operating before reaching 250 profiles did so for a variety of reasons. Some succumbed due to faulty components, including electronics, batteries, and likely O-ring failures. Others might have sustained damage during shipping that was unknown at the time of deployment or malfunctioned due to deployment errors. Additionally, an energy budget such as that shown in Table 2 is derived from measurements performed on only a few laboratory floats. The energy values shown in the second column of the table likely have some presently unknown float-to-float variation; it is assumed that this variation is small compared to the values shown in the table, but the degree of variability between floats is not known and will likely alter the estimated number of profiles based on energy alone.

A suite of 99 UW Argo floats (all using Iridium communications and carrying CTD sensors only) that each spent at least some time under sea ice, a potentially more problematic environment, fared nearly as well as the control Argo group, with half the floats surviving to about 200 profiles and a smaller fraction even longer. For SOCCOM, as is evident in Figure 12, the surviving fraction of floats as a function of profile number is tending generally to parallel the curves for both groups of basic Argo floats, although the SOCCOM ensemble is relatively small, a sizable fraction is near sea ice, and few of the floats have been in the water for longer than about 100 profiles. The SOCCOM floats appear to be performing well and there is ample reason for optimism in these results, although several more years must pass before the accuracy of the laboratory lifetime estimates can be confirmed.

8. Summary and Future Work

The results presented herein show that profiling float technology has matured in the past decade to the point that floats with a variety of BGC sensors can be deployed in a hostile ocean environment (the sea ice regime), and successfully transmit megabytes of data over their lifetime, with survival over many years a likely outcome. This survival has already been demonstrated with certainty for basic Argo floats, and there is good reason to be optimistic that the floats equipped with BGC sensors in SOCCOM will eventually show similar results. The ice avoidance algorithm, a major requirement for success in SOCCOM, has worked well, allowing for unprecedented views of the evolution of physical and BGC variables under wintertime sea ice as discussed by Johnson et al. (2017) and others.

At the present time most of the floats in SOCCOM have been fabricated at the University of Washington from components purchased from Teledyne/Webb Research. This fabrication process requires a dedicated engineering team at UW that, while costly, undoubtedly adds value to the floats and extends their lifetimes significantly. Most of the additional sensors and capabilities beyond those of standard Argo floats have been added and engineered by the UW float group in collaboration with colleagues at MBARI and commercial sensor manufacturers. Yet there is a limit to the numbers of instruments that can be produced in this manner. For SOCCOM, university-based fabrication has worked well, but if the numbers of BGC floats increase as coverage expands beyond the Southern Ocean it will be necessary to use fully commercially available versions.

The successful use of BGC-capable floats raises the question of what else the floats might be able to do. One possible option is to add additional sensors to BGC floats that have already been successfully used on other types of floats. For example, passive acoustic methods have been used successfully to estimate wind speed and rainfall from floats in the tropics and subtropics (Riser et al., 2008; Yang et al., 2015), and there seems to be no fundamental reason why such sensors could not also be added to BGC floats. This capability would allow the mixing and evolution of both physical and BGC variables to be examined in the context of precise local wind measurements in the Southern Ocean region. In a similar context, if an auxiliary, high-resolution, near surface CTD unit could be added to the floats (such as the instrumentation described in Anderson & Riser, 2014), small-scale mixing very close to the sea surface can be studied in a regime that is very different than the tropics where such instrumentation has traditionally been used.

As a central goal of SOCCOM is to understand the carbon cycle in the Southern Ocean, several types of sensors for measuring pCO₂ are now under development and it is hoped that these can be tested on UW-built floats within a few years. Another improvement in estimates of basic carbon parameters in the ocean could come from a small, low-power sensor to measure Total Alkalinity that is presently being developed (Briggs et al., 2017); the performance of this sensor should be evaluated on a profiling float at the earliest possible opportunity.

As noted in Riser et al. (2016), given ongoing developments in float and sensor technology, a decade from now the floats used in BGC studies of the world ocean might be quite different from the technology being used today. Yet making observations in the Southern Ocean, especially in the seasonal ice zone, will surely continue to be a challenging undertaking.

Acknowledgments

The data used in this paper were collected and made freely available by the International Argo Program and the national programs that contribute to it. The Argo Program is part of the Global Ocean Observing System. The data used in this paper are available from the Argo Global Data Assembly Center and have been archived with a digital object identifier (<http://doi.org/10.17882/42182#47708>). We thank our colleagues Rick Rupan, Greg Brusseau, and Andrew Meyer, who carried out the work of actually building the floats discussed in the paper. We also acknowledge many useful discussions with Annie Wong about data quality and the under-ice algorithm. Our colleagues at MBARI, including Ken Johnson, Luke Coletti, and Hans Jannasch designed and built the NO₃ and pH sensors used on the UW SOCCOM floats. We also acknowledge the helpful guidance and inspiration provided by our SOCCOM colleagues Jorge Sarmiento, Lynne Talley, Joellen Russell, and Roberta Hotinski, and all of the other participants in SOCCOM. This work was funded by the National Science Foundation under grant OPP-1429342 and by NOAA through grant NA15OAR4320063.

References

- Anderson, J., & Riser, S. (2014). Near-surface variability of temperature and salinity in the near-tropical ocean: Observations from profiling floats. *Journal of Geophysical Research: Oceans*, 119, 7433–7448. <https://doi.org/10.1002/2014JC010112>
- Briggs, E., Sandoval, S., Erten, A., Takeshita, Y., Kummel, A., & Martz, T. (2017). Solid state sensor for simultaneous measurement of total alkalinity and pH of seawater. *ACS Sensors*, 2, 1302–1309. <https://doi.org/10.1021/acssensors.7b00305>
- Boyer, T., Antonov, J., Baranova, O., Garcia, H., Grodsky, A., et al. (2013). *World Ocean Database 2013* (NOAA Atlas NESDIS 72, 209 pp.). In: Levitus, S., Mishonov, A. (Eds.). Silver Spring, MD: NOAA.
- Bushinsky, S., Emerson, S., Riser, S., & Swift, D. (2016). Accurate oxygen measurements on modified Argo floats using in situ air calibration. *Limnology and Oceanography Methods*, 14, 451–506.
- Chamberlain, P., Talley, Mazloff, L., Riser, S., Speer, S. K., & Gray, A. (2018). Observing the ice-covered Weddell Sea with profiling floats: position uncertainties and correlation statistics. *Journal of Geophysical Research-Oceans*, accepted for publication.
- Davis, R. (2005). Intermediate-depth circulation of the Indian and South Pacific Oceans measured by autonomous floats. *Journal of Physical Oceanography*, 35, 683–707.
- Davis, R., Sherman, J., & Dufour, J. (2001). Profiling ALACEs and other advances in autonomous subsurface floats. *Journal of Atmospheric and Oceanic Technology*, 18, 982–993.
- Hennon, T., Riser, S., & Alford, M. (2014). Observations of internal gravity waves by Argo floats. *Journal of Physical Oceanography*, 44, 2370–2386.
- Iqbal, M. (1983). *An introduction to solar radiation* (408 pp.). Cambridge, MA: Academic Press.
- Johnson, K., Jannasch, H., Coletti, L., Elrod, V., Martz, T., Takeshita, Y., et al. (2016). Deep-sea DuraFET: a pressure tolerant pH sensor designed for global sensor networks. *Analytical Chemistry*, 88, 3249–3256.
- Johnson, K., Plant, J., Coletti, L., Jannasch, H., Sakamoto, C., Riser, S., et al. (2017). Biogeochemical sensor performance in the SOCCOM float array. *Journal of Geophysical Research-Oceans*, 122, 6416–6436. <https://doi.org/10.1002/2017JC012838>
- Johnson, K., Plant, J., Riser, S., & Gilbert, D. (2015). Air oxygen calibration of oxygen optodes on a profiling float array. *Journal of Atmospheric and Oceanic Technology*, 32, 2160–2172.
- Klatt, O., Boebel, O., & Fahrbach, E. (2007). A profiling float's sense of ice. *Journal of Atmospheric and Oceanic Technology*, 24, 1301–1308.
- Kwon, Y.-O., & Riser, S. (2005). The general circulation of the western subtropical North Atlantic observed using profiling floats. *Journal of Geophysical Research*, 110, C10012. <https://doi.org/10.1029/2005JC002909>
- Lavender, K., Davis, R., & Owens, W. B. (2000). Mid-depth recirculation observed in the interior Labrador and Irminger Seas by direct velocity measurements. *Nature*, 407, 66–69.
- Molinari, R., Garzoli, S., & Schmitt, R. (1999). Equatorial currents at 1000 m in the Atlantic Ocean. *Geophysical Research Letters*, 26, 363–363.
- Owens, W. B., & Wong, A. (2009). An improved calibration method for the drift of the conductivity sensor on autonomous CTD profiling float by theta-S climatology. *Deep-Sea Research Part I: Oceanographic Research Papers*, 56, 450–457.
- Riser, S., Nystuen, J., & Rogers, A. (2008). Monsoon effects in the Bay of Bengal inferred from profiling float-based measurements of wind speed and rainfall. *Limnology and Oceanography*, 53, 2080–2093.
- Riser, S., Freeland, H., Roemmich, D., Wijffels, S., Troisi, A., Belbeoch, M., et al. (2016). Fifteen years of observations with the global Argo array. *Nature Climate Change*, 6, 145–153. <https://doi.org/10.1038/NCLIMATE2872>
- Rosby, T., Dorson, D., & Fontaine, J. (1986). The RAFOS system. *Journal of Atmospheric and Oceanic Technology*, 3, 672–679.
- Rosby, T., & Webb, D. (1970). Observing abyssal motions by tracking Swallow floats in the SOFAR channel. *Deep Sea Research and Oceanographic Abstracts*, 17, 359–365.
- Swallow, J. (1955). A neutral buoyancy float for measuring deep currents. *Deep Sea Research*, 3, 74–81.
- Swallow, J. (1971). The AIRE current measurements in the western North Atlantic. *Philosophical Transactions of the Royal Society of London A*, 270, 451–460.
- Swallow, J., McCartney, B., & Milliard, B. (1974). The Minimode float tracking system. *Deep Sea Research and Oceanographic Abstracts*, 21, 573–595.
- Swallow, J., & Worthington, L. (1957). Measurements of deep currents in the western North Atlantic. *Nature*, 179, 1183–1184.
- Swift, D., & Riser, S. (1994). RAFOS floats: defining and targeting surfaces of neutral buoyancy. *Journal of Atmospheric and Oceanic Technology*, 11, 1079–1092.
- Wang, J., Mazloff, M., & Gille, S. (2014). Pathways of the Aghuhas waters poleward of 29 S. *Journal of Geophysical Research: Oceans*, 119, 4234–4250. <https://doi.org/10.1002/2014JC010049>
- Wong, A., Johnson, G., & Owens, W. B. (2003). Delayed-mode calibration of autonomous CTD profiling float salinity data by theta-S climatology. *Journal of Atmospheric and Oceanic Technology*, 20, 308–318.
- Wong, A., & Riser, S. (2011). Profiling float observations of the upper ocean under sea ice off the Wilkes Land Coast of Antarctica. *Journal of Physical Oceanography*, 41, 1102–1115.
- Yang, J., Riser, S., Nystuen, J., Asher, W., & Jessup, A. (2015). Regional rainfall measurements using the Passive Aquatic Listener during the SPURS field campaign. *Oceanography*, 28, 124–133.